

Review

Molecular Activation Mechanism and Structural Dynamics of Orange Carotenoid Protein

Volha U. Chukhutsina * and Jasper J. van Thor * 

Department of Life Sciences, Imperial College London, London SW7 2AZ, UK

* Correspondence: v.u.chukhutsina@vu.nl (V.U.C.); j.vanthor@imperial.ac.uk (J.J.v.T.)

Abstract: Like most photosynthetic organisms, cyanobacteria are vulnerable to fluctuations in light intensity, which can damage their photosynthetic machinery. To protect against this, they use a photoprotective mechanism called non-photochemical quenching (NPQ), where excess absorbed photo-energy is dissipated as heat. In cyanobacteria, light activation of Orange Carotenoid Protein (OCP) is the critical first step in the NPQ response. OCP is also the only known photosensitive protein, which uses carotenoid for its activation. We summarize the current knowledge on the light induced reactions of OCP; the different mechanisms of activation that have been proposed; photocycle kinetics and characteristics; and the reported structural intermediates. We discuss the possible interpretations of reported experimental results, and we formulate important open questions and directions for future work, to reveal the molecular and structural basis of photosensing by OCP.

Keywords: carotenoids; enolization; intramolecular charge transfer; isomerization; orange carotenoid protein; photosensors; photosynthesis



Citation: Chukhutsina, V.U.; van Thor, J.J. Molecular Activation Mechanism and Structural Dynamics of Orange Carotenoid Protein. *Physchem* **2022**, *2*, 235–252. <https://doi.org/10.3390/physchem2030017>

Academic Editor: Ray Luo

Received: 27 May 2022

Accepted: 15 July 2022

Published: 20 July 2022

Publisher's Note: MDPI stays neutral with regard to jurisdictional claims in published maps and institutional affiliations.



Copyright: © 2022 by the authors. Licensee MDPI, Basel, Switzerland. This article is an open access article distributed under the terms and conditions of the Creative Commons Attribution (CC BY) license (<https://creativecommons.org/licenses/by/4.0/>).

1. Introduction

Photosensitive proteins play a crucial role in the life and development of various organisms, from animals to unicellular bacteria, where they regulate a vast range of processes, such as circadian rhythms, organism development, phototaxis and many others [1,2]. Photosynthesis is another process relying on different photosensors and photoreceptors [3]. More than half of the total photosynthesis activity on earth occurs in single-celled organisms, especially algae and cyanobacteria. Therefore, cyanobacteria are excellent model organisms to study the efficiency and regulation of light energy harnessing and storage. During their evolution, photosynthetic organisms have evolved various photoprotective strategies to cope with fluctuating light intensity and quality, as well as other environmental stresses, by adjusting their photosynthetic machinery. Adaptation to rapid environmental changes is crucial for maintaining optimal photosynthetic efficiency, and is ultimately key to their survival. Most photosynthetic organisms protect their photosynthetic apparatus against rapidly increasing light intensities using non-photochemical quenching (NPQ): a mechanism by which excess photo-energy is dissipated as heat [4,5]. This response is rapid (minutes or less) and does not involve changes in gene expression, but instead requires a rapid functional switch of the photosynthetic machinery from a “light-harvesting” into a “heat-dissipating” state. In cyanobacteria, this is controlled by a unique photosensitive protein, Orange Carotenoid Protein (OCP) [6]. OCP is the only known photoreceptor protein which uses a carotenoid for its activation. Because of its unique structure and importance, it is vital for the scientific community to fully understand how this carotenoid-based light-activation process is activated, and subsequently controls NPQ in cyanobacteria. These goals require an understanding of the initial activation mechanism, the intermediate and final structural states, and the kinetics of the OCP photocycle. However, following important spectroscopy and structural studies over the last decade, many of the fundamental questions still need to be answered. Therefore, there is a strong need to summarize

and discuss all the progress and evidence from structural and time-resolved spectroscopic studies, and give directions for future work. This is the aim of this review.

2. Structure and Function of OCP

OCP is a water-soluble protein composed of two domains: an all-helical N-terminal domain (NTD, residues 15–165- annotation is based on PDB ID code 5TV0) that is unique for cyanobacteria; and a C-terminal domain (CTD, residues 190–317), which is an α/β -fold domain of the ubiquitous Nuclear Transport Factor-2 (NTF2) superfamily, also found in many other organisms (Figure 1). The structure of the C-terminal domain resembles blue-light responsive BLUF and LOV domains, which also contain a core β -sheet surrounded by helices [6]. The two domains are joined together by: (1) an N-terminal extension (NTE, residues 1–15), packing against the central β -sheet of the CTD; (2) a flexible linker between the two domains running on the molecular surface opposite the NTE (residues 166–189) [7]; (3) salt bridge between Arg155 and Glu244; (4) by keto-carotenoid buried inside the two domains (Figure 1a,b).

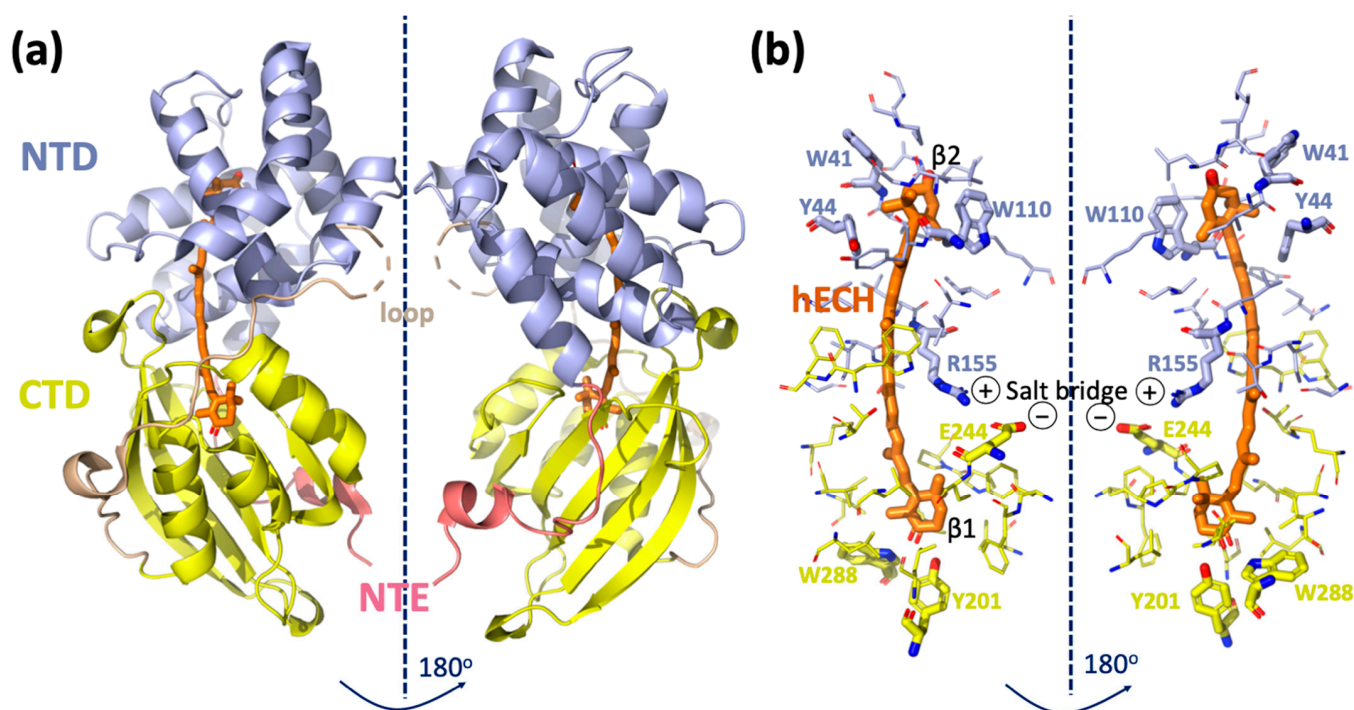


Figure 1. Structure of Orange Carotenoid Protein. (a) Crystal structure of *Synechocystis sp. PCC6803* OCP (PDB ID code 5TV0) consisting of two domains, NTD and CTD, NTE and the loop as described in the main text introduction. (b) Amino acid residues within 4.5 Å of the carotenoid are shown by sticks.

To protect themselves against fluctuating light intensities, cyanobacteria can adjust energy flows through their photosynthetic antenna complexes, the phycobilisomes (PBSs). OCP plays a crucial role in this process. Absorption of blue–green light by the keto-carotenoid induces conformational changes in the carotenoid and the protein, converting stable inactive OCP^O (the so-called orange form) into unstable but active OCP^R (red form), which is also followed by drastic changes in the OCP absorption. It is known that only OCP^R can bind to PBSs and induce NPQ [8,9]. OCP^R could potentially quench excitation energy either directly or indirectly (see the proposed mechanisms [10–12] and the recent review [13]).

3. Role of Individual Amino Acids in OCP Light Activation

For OCP to be photoactive, a keto-carotenoid should be present in the middle of its structure (Figure 1). The OCP has been shown to bind and be active with various keto-carotenoids (3-hydroxyl-echinenone, hECN; echinenone, ECN; and canthaxanthin, CAN) [14–16]. All of these are composed of a conjugated chain of 11 carbon–carbon double bonds, which are in all trans configuration in OCP^O, and a keto-group. The keto-group is located in CTD in the β1-ring of the keto-carotenoid. It is involved in a hydrogen bond formation between the keto-carotenoid and the protein moiety. The latter is supplied by the hydroxyl group of Tyr201 and the amino group of Trp288, both located in CTD (Figure 2). The other ring of the carotenoid (β2) is nestled within a group of conserved aromatic residues (Trp41, Tyr44, Trp110) in the NTD (Figure 2) [7]. Multiple mutagenesis studies narrowed down the list of amino acids playing a crucial role in OCP function (Figure 2): If Tyr201 or Trp288 gets mutated, the OCP^R is not accumulated; therefore, OCP activity is considered to be lost [17]. In addition, these amino acids are responsible for carotenoid affinity and specificity [18].

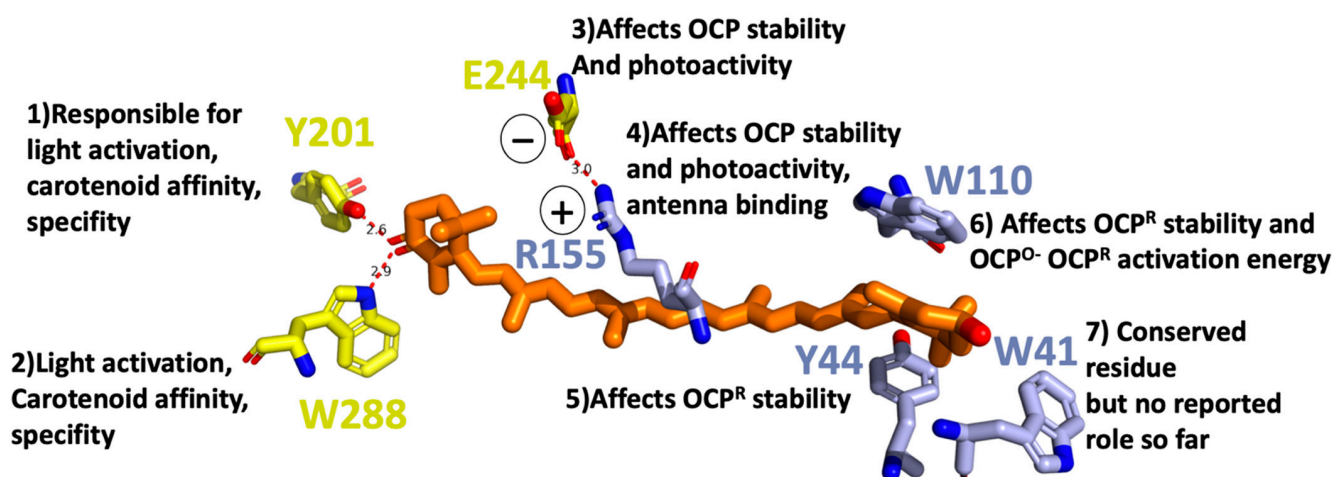


Figure 2. Tentative role of individual amino acids in OCP light activation in a close Car vicinity based on mutagenesis studies [17–19].

If Tyr44 is replaced by Ser, OCP^R is also not accumulated at any temperature indicating Tyr44, an essential role in OCP light activation process. On the other hand, the replacement of Trp110 by Ser affects the activation energy, necessary for the OCP^O to OCP^R conversion. Replacement of Tyr44 and Trp110 with Phe does not affect the OCP^R accumulation, demonstrating the critical function of the aromatic rings of the side chains in the OCP photocycle [19]. Other site-directed mutagenesis studies demonstrated that salt bridge between Arg155 and Glu244 stabilizes the interaction between the N- and C-terminal domains: its disruption increased the rate of photoactivity and the stability of the photoactivated OCP^R [18]. Changing Glu244 to Leu had no effect on OCP binding to PBS. By contrast, substitution of Arg155 with a neutral or a negatively charged amino acid largely decreased OCP binding to the PBs, whereas substitution with a lysine slightly perturbed the interaction. Based on that finding, it was suggested that the surface of the N-terminal domain, containing the Arg155, is the place where OCP binds/interacts with the PBS.

The specific roles or functional associations of different amino acids in the light activation process, or in NPQ, indicate that light activation and photoprotection are not interconnected processes, although some amino acids could play a dual role. Since many amino acids have a direct effect on light activation, the process must be driven by a cascade of protein-conformational changes, initiated by carotenoid light-absorption. This cascade of events will be discussed in the next section. Further discussion of the possible quenching mechanisms of PSBs by OCP has been presented previously [13].

4. OCP^O Versus OCP^R

4.1. Global Structural Changes

The molecular weight (MW) of OCP^O was originally measured to be 34.6 kDa by matrix-assisted laser desorption/ionization mass-spectrometry (MALDI-MS) and electro-spray techniques, and was later confirmed by the resolved X-ray structure [7,20], while the MW of OCP^R is still under debate. Solution studies using small angle X-ray scattering (SAXS), and dynamic light scattering, demonstrated a large difference in the global structure of OCP^O and OCP^R, with OCP^R showing a ~30% and ~50% increase in the radius of gyration and maximal dimension, respectively [21]. In all studies, size exclusion chromatography (SEC) of OCP^R gives an earlier eluting peak than for OCP^O, indicating a larger hydrodynamic volume for OCP^R [21,22]. Leverenz and co-workers predicted globular mass of 43 kDa, while Gupta and co-workers found it to be 63 kDa. The discrepancy is intriguing and seems to arise from different illumination protocols. Different illumination schemes were used in these two studies, suggesting that the resolved MW might correspond to MW of different intermediates from the OCP^O-OCP^R photocycle. But more importantly, both studies observed an increase in various measurements of the OCP^R size, as compared to OCP^O.

Far-UV CD measurements reveal global changes in secondary structure of OCP upon light illumination [23,24]. Comparison of far-UV CD measurements in OCP^O and OCP^R demonstrate only minor changes in CD signal, indicating that the secondary structure of OCP^R is hardly different from OCP^O [21,22]. Using several algorithms to calculate the predicted secondary structure of OCP^O and OCP^R, from the experimental far-UV CD curves, Gupta et al. interpreted minor changes as loss of only a small portion of the protein's α -helical structure (2% α -helical content = ~6 residues) after illumination [21]. Mass spectrometry foot printing revealed that salt bridging between R155 and E244 weakens or completely disrupts during OCP^O to OCP^R transition. All these results point towards CTD and NTD separation [21,22,25].

Keto-carotenoids are nearly symmetric, and thus, normally inactive as seen by VIS CD [26]. However, the binding of a keto-carotenoid to the protein introduces asymmetry into the chromophore, giving rise to a VIS CD signal. The VIS CD spectra of the OCP^R are substantially lower than OCP^O, suggesting that CTD from NTD separation upon light activation causes lowering of keto-carotenoid asymmetry, and less protein–chromophore interactions [27]. There have so far been no successful attempts to obtain crystal structures of the fully active OCP^R form to unambiguously resolve the change in protein–chromophore interactions after light activation. However, it was discovered that NTD as a truncated fragment can bind keto-carotenoid, giving rise to red carotenoid protein (RCP) [15,22]. Comparisons between the crystal structures of OCP and RCP has led to a recent proposal that carotenoid undergoes a 12-Å translocation relative to the protein framework, in forming photoactivated OCP^R [15]. However, it is important to learn whether the 12-Å carotenoid translocation occurs in a native OCP^R, which steps of structural events trigger such a substantial change in keto-carotenoid coordinates, and, in particular, how it affects the protein structure and protein binding interface.

To summarize, OCP^R represents a molten-globule state, the intermediate of protein folding (Figure 3), which has a secondary structure similar to the native form. This state is characterized by CTD and NTD domain separation, caused by modifications of carotenoid-protein interactions, and as a result, salt bridge disruption and detachment of the α A helix [21,28].

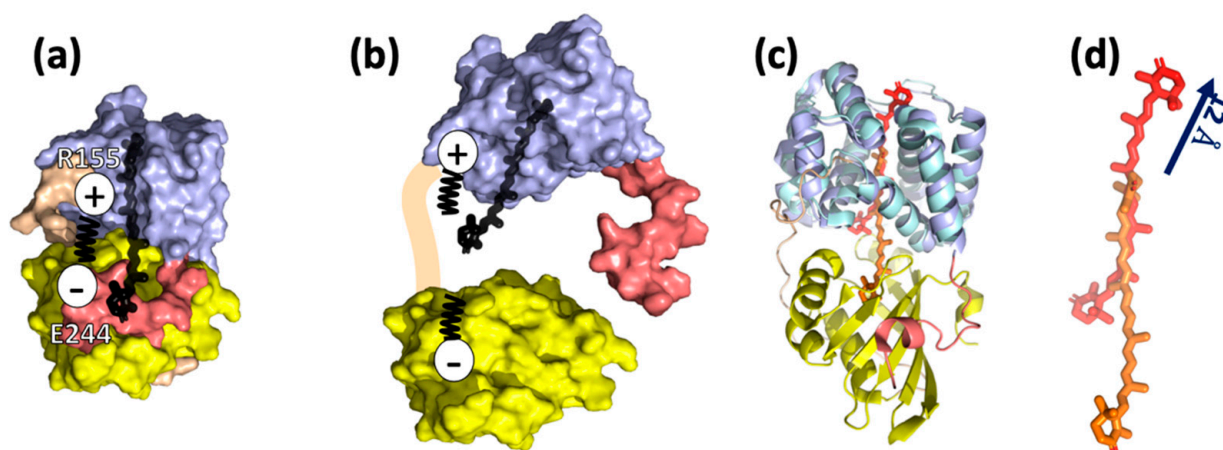


Figure 3. Current knowledge on OCP^R structure. (a) Crystal structure of *Synechocystis* sp. PCC6803 OCP^O (PDB ID code 5TV0) consisting of two domains, NTD and CTD, NTE and the loop as shown in Figure 1. The salt bridge R155-E244 plays an important role in connecting the two domains. (b) The model of OCP^R by Leverenz et al. [15,22]: NTD and CTD are partially or entirely separated, promoted by salt bridge disruption, and keto-carotenoid is translocated into NTD [21]. (c) Comparison of OCP^O (5TV0, coloring according to Figure 1) and RCP (amino acids and the keto-carotenoid are colored with cyan and red, respectively). (d) Superposition of NTD and RCP demonstrates 12 Å translocation of keto-carotenoid inside the protein network. This translocation is considered to be present in OCP^R [15].

4.2. Changes in the Secondary and Tertiary Structure

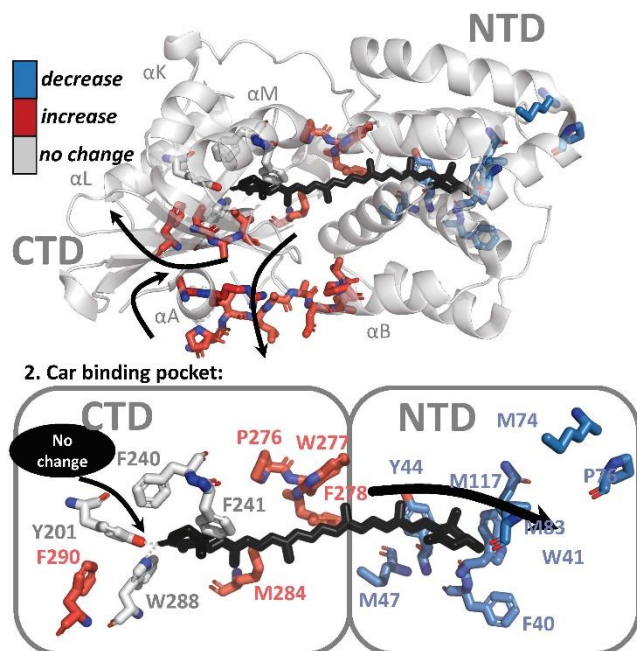
Two structural approaches were used to resolve changes in the secondary and tertiary structure of OCP, upon illumination. Hydrogen/deuterium Exchange Mass Spectrometry (HDX-MS), together with X-ray protein foot printing (XF-MS), were used to resolve solution phase protein conformation and differences [21]. This study was later complimented, with the first result demonstrating structural changes on an atomistic level, using X-ray crystallography in illuminated OCP crystals [16]. X-ray protein foot printing (XF-MS), and HDX-MS techniques, demonstrate that activation of the OCP results in disruption of the minor interface, the interaction between the N-terminal α -helix and the solvent-exposed β -sheet of the CTD, via the unfolding of the α A (NTE): XF-MS showed a significant increase in accessibility in OCP^R relative to OCP^O at the minor interface; NTD residues A8–R9 and P13–P22 on the loop joining α A to α B by, commensurate with the corresponding residues V301–A302–I303 on the surface of the β -sheet facing helix α A. High water mobility was also observed. Two clusters of highly mobile waters are centered on the domain interface and close to β 2-ring, playing a role in domain separation (Figure 4a).

Furthermore, a substantial decrease in solvent accessibility upon illumination was observed at residue clusters, which are in the carotenoid vicinity in NTD (W41–Y42–Y44, M47, M74–P76–M83, and M117), concomitantly with an increase in solvent accessibility in CTD residue clusters surrounding carotenoid in CTD (P276–W277–F278–M284 and F290), supporting the hypothesis of carotenoid translocation from CTD to NTD during light activation [15]. However, surprisingly, residues involved in H-bonding with the β 1-ring of keto-carotenoid, Trp-201 and Tyr-288, were absolutely conserved in solvent accessibility, suggesting that H-bond is still present in the illuminated state. Furthermore, residue Phe-240, which projects toward the β 1-ring of carotenoid, and Phe-241, which projects toward the core of CTD, also showed no modification. These observations raise an important question: the XF-MS and HDX-MS results suggest that even if the translocation (partially) occurs during OCP^O to OCP^R transition, it should not be substantial, since the hydrogen bond between β 1, Tyr-288 and Trp-201 appears to remain and would not be ruptured in OCP^R. An alternative explanation is that the illuminated state in the study is not the final

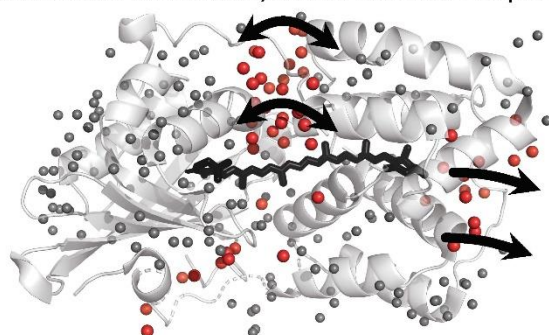
OCP^R state, suggesting that H-bond rupture is not the primary photoactivation event, but occurs as a result of domain separation in later stages.

(a) Change in solvent accessibility in OCP^R *ref 21*

1. Disruption of α A and CTD interface via α A unfolding

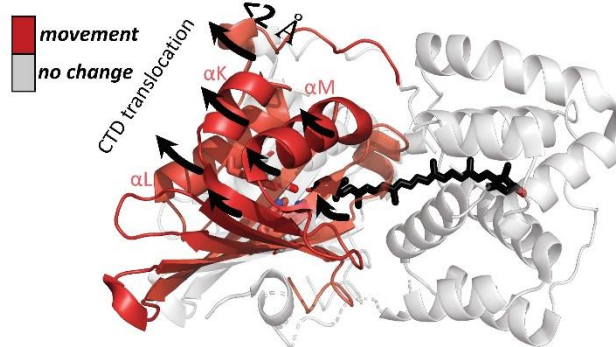


2. Car binding pocket:



(b) OCP^R vs OCP^O in crystalline *ref 16*

1. Up to 2 Å translocation of CTD away from NTD



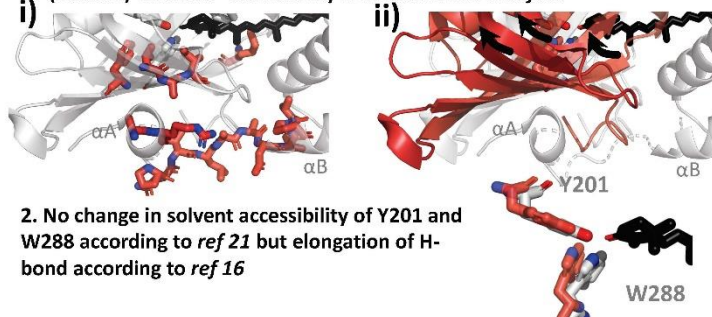
2. The H-bond gets larger: H-bond rupture is suggested



(c) Major variations of the two studies

1. (insert i) Increase in solvent accessibility and α A unfolding observed in *ref 21*.

(insert ii) However α A mobility is not observed in *ref 16*



2. No change in solvent accessibility of Y201 and W288 according to *ref 21* but elongation of H-bond according to *ref 16*

Figure 4. Summary of light-induced structural changes in OCP resolved by HDX-MS and XF-MS [21], and X-ray crystallography [16]. (a) Structural changes as resolved by HDX-MS and XF-MS [21]. The amino acids which showed an increase and decrease in solvent accessibility are colored in blue and red, respectively. Amino acids which showed no change in solvent accessibility are colored in grey. (b) Structural changes as resolved by T-scan X-ray crystallography [16]. Amino acids showing movement in illuminated crystals are colored in red. (c) Summary of the differences of the two studies.

Recently, Bandara and co-workers demonstrated for the first time that OCP could be light-activated in the crystalline state, by showing Fourier difference maps between dark and light states (the crystals were illuminated for 10–15 min at cryo temperatures 100–180 K). While structural differences were demonstrated, the crystals did not show UV/VIS spectroscopic differences upon illumination. This important result provided further opportunities for more in-depth studies of OCP using crystallography. The authors observed that difference densities were mostly localized in CTD, suggesting that CTD is the primary domain responsible for structural rearrangements. In contrast to the small-amplitude movement in NTD (<0.8 Å), CTD underwent significant atomic displacements (as large as 2 Å) in a direction away from NTD and the dimer interface (Figure 4b). Three helices (α K, α L and α M) and the central β -sheet of CTD move together like a rigid body,

away from the NTD. As a result of that movement, hydrogen bonds from the 4-keto group to Tyr201 and Trp288 become longer by 0.2–0.4 Å. Both the raw and SVD-filtered difference maps show evenly spaced positive and negative difference densities associated with carotenoid, suggesting a small shift roughly along the conjugated plane of the polyene chain. The authors also observed movements associated with water molecules at the dimer interface, where a network of hydrogen bonds and the Arg155–Glu244 salt bridge are altered. Based on the elongation of the H-bond by 0.2–0.4 Å, the authors proposed that the H-bond eventually gets ruptured, possibly due to the shift in keto-enol equilibrium; however, it could be a secondary effect resulting from domain separation, in agreement with observations from Gupta et al. [21].

Both structural studies showed a separation of CTD from NTD, which was observed together with the presence of highly-mobile water molecules at the dimer interface [16,21]. This interface also played a role in domain separation and the modification of the Arg155–Glu244 salt bridge. In the work of Bandara and co-workers, this process is not accompanied by unfolding of α A [16], unlike reported by Gupta et al. [21]. Since large scale protein and/or cofactor movements would be restrained by crystal lattice, the OCP^R state in crystalline likely resembles an intermediate state of the OCP^O-OCP^R photocycle in solution. All in all, there are some discrepancies between the results of structural studies of OCP activation [16,21]; a full structural mechanism and determination of intermediates is still lacking.

5. OCP^O-OCP^R-OCP^O Photocycle

The structural studies reported above aimed to unravel the structural differences between OCP^O and OCP^R, but did not provide dynamics and kinetics information for these changes. Time-resolved spectroscopy has been an established technique in studying kinetics of the photoactivation and relaxation processes within photosensitive proteins [29–32]. One of the main technical difficulties in applying time-resolved spectroscopy techniques for OCP research is the very low OCP^O-OCP^R conversion efficiency (1–3%) [8,33], and quite long OCP^R-OCP^O relaxation time (minutes). To overcome these issues, either relatively long excitation pulses (from several ps to ns) or continuous illumination should be used, in combination with efficient sample refreshment using a Lissajous sample scanner, or flow-through cuvette.

5.1. Flash Photolysis

Maksimov and co-workers reported the first study of the OCP^O-OCP^R-OCP^O photocycle with subsecond resolution [33]. They performed nanosecond flash photolysis to monitor hECN absorption changes, as well as protein structural changes. The latter was probed by time-resolved Trp autofluorescence measurements, and time-resolved fluorescence measurement of Nile Red label, the hydrophobicity reporter dye. The OCP^O to OCP^R transition, as seen by 550 nm OD changes, was single exponential and its rate was recorded to be flux-dependent, while OCP^R-OCP^O relaxation in darkness was biexponential. The characteristic relaxation times were 13 s and 66 s with an amplitude ratio of 3:1 in the region between 20 and 45 °C, and of 3:2 at lower temperatures (5–17 °C) [33]. Changes in OCP^O-OCP^R-OCP^O kinetics, as monitored by OD change recorded at 550 nm OD, followed the changes in Trp fluorescence yield [33]. This correlation suggested the principal role of carotenoid-protein interactions or, at least, carotenoid-Trp interactions in the formation of OCP photocycle. From these measurements it is not possible to determine which Trp contributes to these dynamics and assign these signals to actual structural intermediates. Time-resolved Trp measurements in the ns range demonstrated an increase in the average lifetime and amplitude of OCP^R, as compared to OCP^O. The difference between the two fluorescence traces can be fit monoexponentially with 5 ns lifetime, indicating that only one type of fluorescent Trp interaction plays a role during OCP^O-OCP^R-OCP^O conversion. It is accompanied with a 3 nm blue shift of the Trp spectral band in the OCP^R state, indicating changes in the local Trp environment. These changes in Trp fluorescence during OCP^O-OCP^R-OCP^O followed

NR fluorescence quenching and recovery; therefore, the $\text{OCP}^{\text{O}}\text{-OCP}^{\text{R}}\text{-OCP}^{\text{O}}$ photocycle also involves some hydrophobic areas getting exposed, then concealed. Recently, the same authors resolved two additional timesteps and assigned them to actual intermediates in the OCP photocycle [34]. The first one is an intermediate $\text{OCP}^{\text{O}}\text{-OCP}^{\text{R}}$ state $\gg 200$ ns (below instrument resolution). This intermediate is assigned to a protein conformation close to OCP^{O} , but carotenoid is in its final red state, according to hECH absorption measurements; however, no Trp autofluorescence could be reported for this state, due to instrument limitations, which could confirm the protein-conformation assignment. The authors also resolved a recovery step of 3 s, when NTD and CTD are properly oriented against each other (likely to be assisted by Fluorescence Recovery Protein *in vivo*), as concluded from the combination of hECN absorption changes and Trp autofluorescence transients. The authors suggest that this step is a prerequisite for the hydrogen bond formation between Tyr-201 and Trp-288, and the keto-group of carotenoid [34]. The knowledge of the $\text{OCP}^{\text{O}}\text{-OCP}^{\text{R}}\text{-OCP}^{\text{O}}$ photocycle, based on the flash photolysis studies [33,34], is summarized in Figure 5.

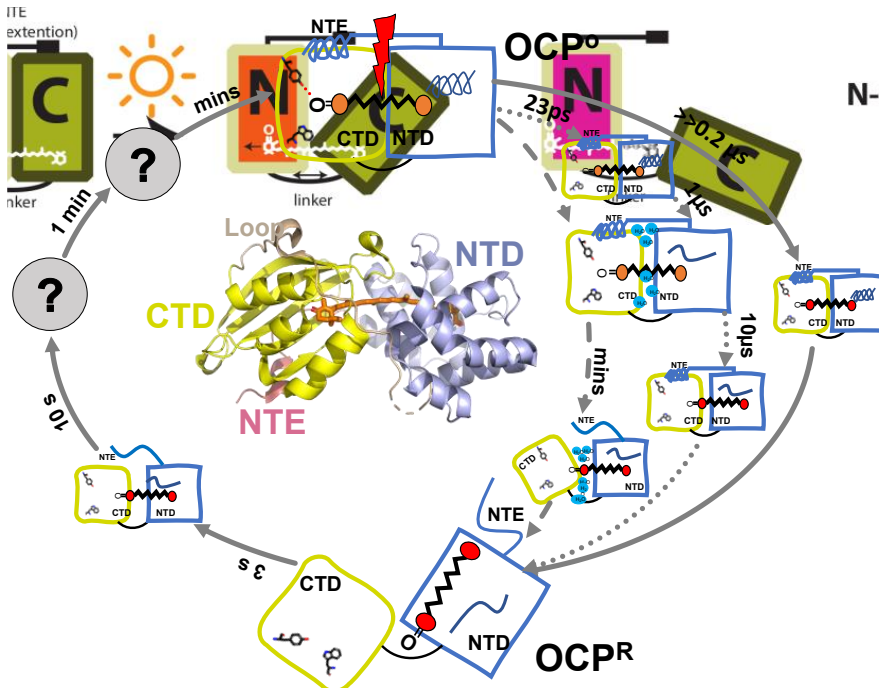


Figure 5. Summarized model of OCP photocycle based on available time-resolved spectroscopic results. Time steps resolved by different techniques are presented by different arrows: flash photolysis [33,34] (solid line); transient absorption [35] (dotted line); FTIR [36] (dashed line).

5.2. Intermediates Resolved by Transient Absorption Spectroscopy and FTIR

Konold and co-workers, using femtosecond to microsecond visible, and infrared transient absorption spectroscopy for the first time, were able to identify ultrafast structural intermediates (in ps- μ s range) in the $\text{OCP}^{\text{O}}\text{-OCP}^{\text{R}}$ pathway, which had not been observed before [35].

The first structurally defined intermediate rises in 23 ps and is characterized by a replacement of 1685 cm^{-1} bleach, which is present at 5 ps and assigned to C=O stretch of $\beta 1$ -ring, by a smaller stretch mode at 1680 cm^{-1} (Figures 5 and 6a). This 5 cm^{-1} shift and loss in intensity were assigned to the loss of a hydrogen bond between keto-group, and Trp-288 and Tyr-201. This assignment is based on previous findings suggesting that OCP light activation is triggered by H-bond rupture between the keto-group of $\beta 1$ ring and the two amino acids [16], and on the assumption that C=O stretch in OCP is substantially red shifted than in the solution, due to strong bonding [35,37]. The next state arises in 0.5–1.1 μ s and manifests itself with a broad and strong bleach centered around 1655 cm^{-1}

with no downshift upon H/D exchange, with shoulders near 1680 and 1635 cm^{-1} , and nearly zero amplitude elsewhere (Figure 6a). Due to the spectra, and the fact that the band is still present in ΔNTE mutant, it was assigned to amide I band, arising from the loss of nonsolvent-exposed α -helix. The authors assign it to the NTD. In 10 μs a formation of the red carotenoid state is observed, which is characteristic for OCP^{R} , but it is not accompanied by any changes in the IR region; therefore, this state affects only Car conformation and not the protein environment. Based on the proposed hypothesis of the carotenoid 12 Å translocation into NTD as a result of OCP^{R} conversion, Konold and co-workers suggest that this OCP “red” state can be explained by carotenoid translocation into NTD.

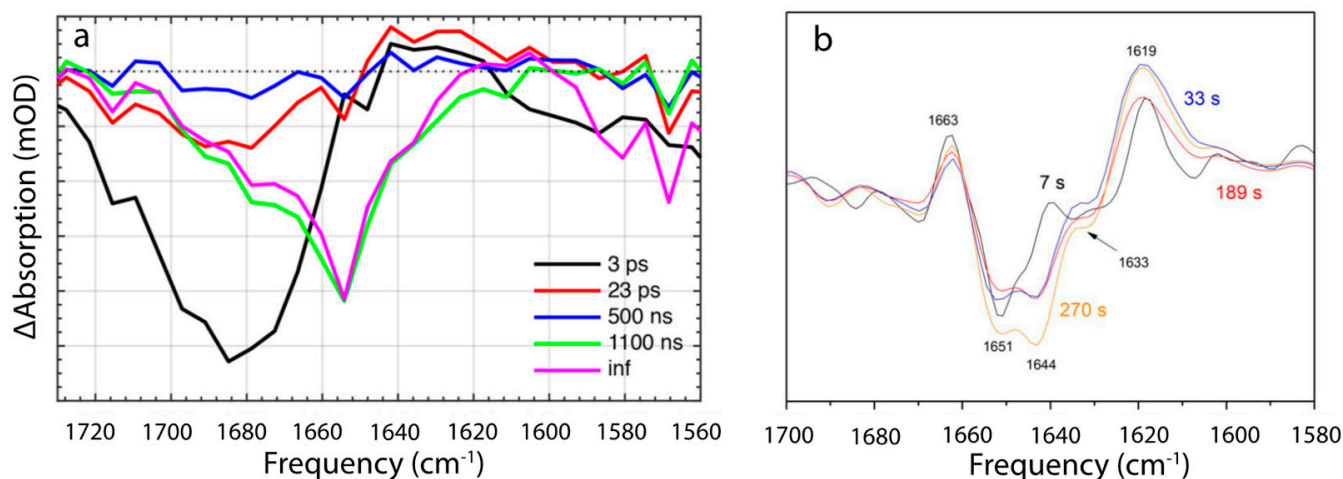


Figure 6. IR time-resolved signals of OCP photocycle [35,36]. (a) Evolution-associated difference spectra determined from global analysis of IR transient absorption data, where ps pulses were used to initiate the OCP photocycle. Reprinted with permission from [35]. Copyright© 2018 American Chemical Society. (b) FTIR difference spectra recorded during continuous illumination at different times after light onset. Reprinted with permission from [36]. Copyright© 2019 American Chemical Society.

Recently, details of the $\text{OCP}^{\text{O}}\text{-OCP}^{\text{R}}\text{-OCP}^{\text{O}}$ photocycle were studied by the time-resolved FTIR Difference spectroscopy study, under continuous illumination [36]. Because of continuous illumination, intrinsic lifetimes cannot be assessed directly, but the measurements do resolve the change in population accumulation rates at given illumination power densities. The authors found two different conformational states during OCP^{O} to OCP^{R} conversion: The first process dominates in the beginning, after the onset, and involves partial reorganization of nonsolvent-exposed α -helix, having a vibration band at 1651 cm^{-1} (Figure 6b), which is virtually identical to the 1655 cm^{-1} contributing to the 0.5–1.1 μs -step resolved by Konold et al. [35]. In both cases the process was assigned to unfolding of the α -helix in NTD. On the same timescales, a positive band at ~ 1619 cm^{-1} of unknown identity was resolved, which, based on the analysis of difference spectra recorded in H_2O and D_2O , was tentatively assigned to movement of water molecules, which may play a key role in the photoactivation mechanism, according to XF-MS, HDX-MS and crystallographic results. The second step becomes dominant later, manifesting itself with 1644 cm^{-1} bleach, and involves a solvent-exposed α -helix. Therefore, it was assigned to NTE.

5.3. Open Questions

The summarized knowledge, based on different spectroscopic studies regarding $\text{OCP}^{\text{O}}\text{-OCP}^{\text{R}}\text{-OCP}^{\text{O}}$ photocycle, is presented on Figure 5. The key questions currently discussed in the literature regarding OCP photocycle are: (1) the time when the OCP^{R} photoproduct is formed and; (2) what mechanism is causing its red shift. Konold et al. observed the photoproduct formation in 10 μs after excitation, but it is not accompanied by any detectable changes in the IR region; therefore, they assign it to carotenoid translocation into NTD [35]. Maksimov and colleagues, however, report the red state of carotenoid to be

formed $\gg 200$ ns, and assign it to the hydrogen bond rupture between Tyr-201, Trp-288 and the keto-group of $\beta 1$ ring, while protein conformation is suggested to be close to OCP^O [34].

Konold et al., on the other hand, suggest that this H-bond rupture occurs in 23 ps and is manifested by a loss of 1685 cm^{-1} band and its 5 cm^{-1} downshift, while no changes in visible spectrum seem to be associated with this state [35]. The presence of the 23 ps time constant that shows spectroscopic differences at 1680 cm^{-1} character, raises questions and requires additional investigation, to confirm its assignment to C=O stretch and H-bond rupture of the keto-group in the $\beta 1$ ring, since IR studies on isolated ECH in solution report different absorption frequencies for C=O stretch [38,39]. The assignment of certain IR frequencies to specific structural rearrangements is challenging, particularly with large protein structures. Therefore, it will be necessary to investigate and exclude the possibility of other pigment-protein interactions contributing to the 23 ps state, for example, a light activation mechanism located in the $\beta 2$ ring, according to recent findings [40] or other proposed trigger mechanisms (see Section 6).

Both IR TA and FTIR studies observe bleach of $1651\text{--}1655\text{ cm}^{-1}$ upon OCP light activation, which is assigned to (partial) unfolding of nonsolvent-exposed α -helix, most likely in NTD. However, far-UV CD, demonstrated loss of only a small portion of the protein's α -helical structure (2% α -helical content = ~ 6 residues) after illumination, which was assigned to NTE based on HDX-MS and XF-MS results, while NTD stayed mainly unchanged, except for minor changes of amino acids in the carotenoid vicinity [21]. Due to this variation in IR and HDX/XF-MS signatures, it is very inviting to consider whether the bleach of $1651\text{--}1655\text{ cm}^{-1}$ upon OCP light activation is actually a signature of α -helix unfolding, or some other change in the secondary or tertiary α -helix structure in NTD or CTD.

6. The Mechanism and Trigger of Light Activation

Most research groups have concluded that OCP photoactivation is initiated by H-bond rupture [15,16,18,19,35,41]. This proposed mechanism is partially based on multiple mutagenesis studies, demonstrating that upon Tyr-201 or Trp-288 mutation in the mutated OCPs, although still binding keto-carotenoids, OCP^R cannot be accumulated [16,17]. Partially, it is also based on the difference maps obtained from dark and illuminated crystals, where the distance between the 4-keto group to Tyr201 and Trp288, becomes longer by $0.2\text{--}0.4\text{ \AA}$ upon illumination.

There are still two important questions which need to be answered: (1) What is the driving force behind this H-bond rupture? (2) Is H-bond rupture the first light activation reaction? Bandara and co-workers hypothesized that keto-carotenoid illumination results in a shift in the keto-enol equilibrium, which weakens or disrupts the hydrogen bonds between the $\beta 1$ ring and protein moiety (Figure 7). The proposed enolization mechanism implies $sp^2 \rightarrow sp^3$ orbital transition at the C6 position of the carotenoid, which was not directly observed in the difference maps. However, crystal structures were obtained after 10–15 min of illumination; therefore, transient signals, if present, could not be resolved. Another proposed mechanism of H-bond rupture concerns photo-induced *s*-isomerization of the C6–C7 single bond, which would flip the orientation of the $\beta 1$ -ring by 90° , going from an *s*-trans to an *s*-cis conformation. Such photo-induced isomerization mechanisms, which rupture or rearrange hydrogen-bonding networks, are commonly in effect in photoreceptor proteins, such as microbial rhodopsins, photoactive yellow protein, and phytochromes [42–44]. Support for such a mechanism in OCP came from X-ray structure of the isolated N-terminal domain (also known as red carotenoid protein, RCP) where keto-carotenoid was present in a C6–C7 *s*-cis conformation [15], and from resonant Raman spectroscopy, where such a conformation would be one of the structures consistent with OCP^R Raman spectra [39]. DFT calculations suggest that there are three additional metastable configurations of the terminal ring, which retain hydrogen bonding to Trp and Tyr, with varying C6–C7 dihedral angles (50° , 80° , 130°) between the polyene chain and the $\beta 1$ -ring [33]. The energy barrier for a $\beta 1$ -ring rotation from 130° to 50° is identical to the value of activation energy

(1.7 kcal/mol at high temperatures), estimated from Arrhenius plots during $\text{OCP}^{\text{O}}\text{-OCP}^{\text{R}}$ photoconversion [33]. The change of torsional angle of the β ring in lutein was recently suggested to be responsible for alternation of the carotenoid energetic landscape, to trigger quenching mechanism in plants [45]. In contradiction to these conclusions, Raman optical activity experiments from Konold and co-workers essentially demonstrated identical anisotropy for OCP^{O} and OCP^{R} states (0.23 and 0.20, respectively), showing that the angle (Θ) between electronic and vibrational transition dipoles states is around the same in both states. It is therefore likely that carotenoid should stay in C6–C7 trans conformation. Based on femtosecond transient absorption data, Konold and co-workers suggest that a specific carotenoid state, typically denoted as the S^* state, is the key state leading to disruption of hydrogen bonds [35]. The S^* state of long (having more than 11 conjugated C=C bonds) carotenoids is either related to structurally distorted form of the optically forbidden state S_1 [35], or to a hot carotenoid ground state that dissipates its energy to vibrational modes of the amino acids near carotenoid [46]. Two recent time-resolved spectroscopic studies also proposed the existence of the S^* state as a precursor of the first OCP photoproduct [47,48]. In addition, both works also observed carotenoid cation formation. The increase of the S^* formation yield seems to go in parallel with cation increase upon UV excitation [47]. However, Niziński and co-workers demonstrate the opposite phenomenon, where OCP photoproduct and cation formation are two decoupled phenomena, upon VIS light excitation [48]. Therefore, it is likely that the S^* and cation formation play different roles in OCP function.

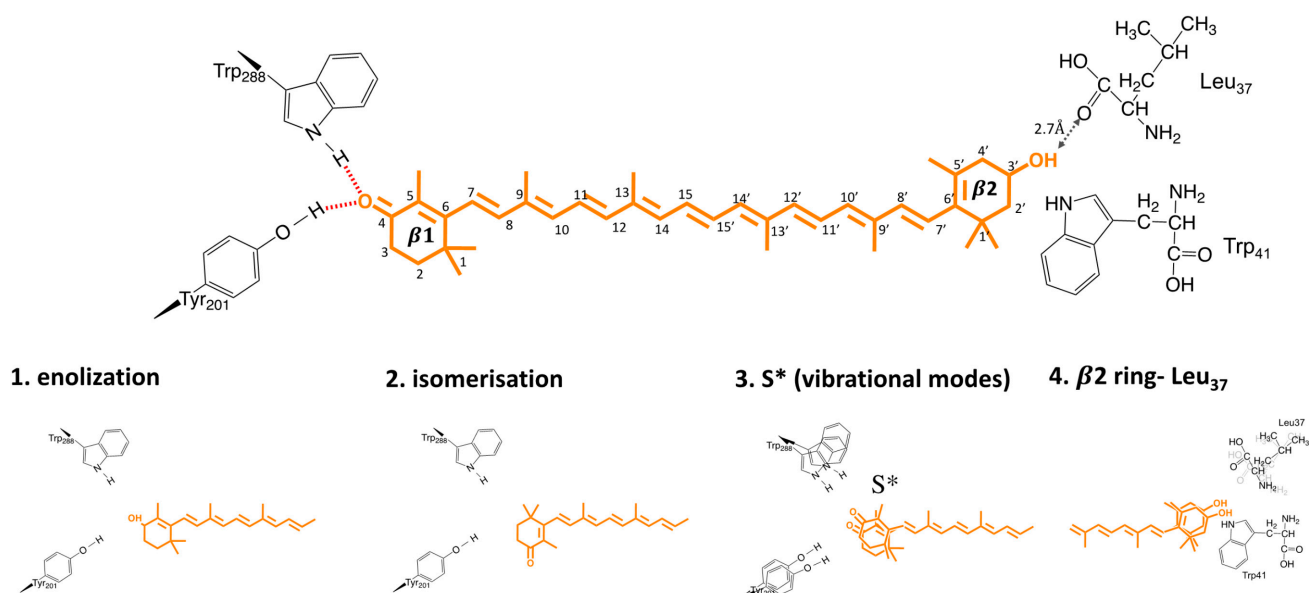


Figure 7. Possible triggers for OCP photosensing (see Section 6 for details).

HDX/XF-MS study suggests that H-bond rupture is not the primary event of OCP light activation and, therefore, S^* -unrelated, but occurs after domain separation [21]. In line with that, by studying fluorescence line shapes, quantum yields, and system–bath couplings in hECN and CAN in OCP^{O} , Gurchiek et al. suggested that the fluorescence spectra and yields and, therefore, S_2 potential surface, are controlled by friction and are modulated by specific interactions of the β_2 rings with Leu37 in the NTD of OCP^{O} . It would suggest that the mechanism of OCP photoactivation is β_1 -insensitive, and involves out-of-plane motions of the β_2 ring.

7. OCP Excited State Dynamics

A range of time-resolved spectroscopic studies have been performed over the last 15 years to describe the energetic landscape of OCP in its two conformations (OCP^{O} and OCP^{R}), and in RCP [49–53]. The structural mechanism of activation is expected to be

initiated via the S_1/ICT ($2^1 A_g^-$) dark state that is created in 150 fs from the optically allowed S_2 ($1^1 B_u^+$), and has a 3.5 ps lifetime [49] (Figure 8).

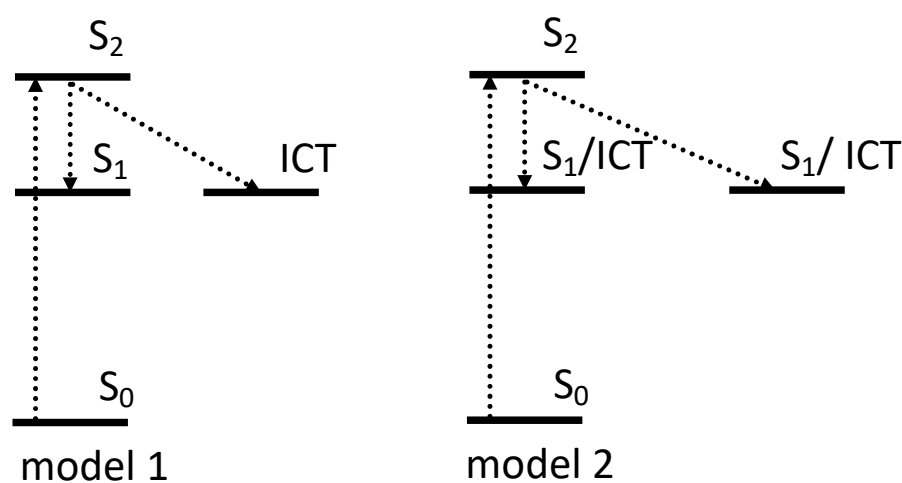


Figure 8. Two schematic models of the excited state dynamics of carotenoid in OCP. The first model assigns the multiexponential character of the S_1 excited state in OCP to the different contribution of ICT in excited state kinetics [49–51], while model two shows OCP population heterogeneity [50,52,53]. The origin and contribution of S^* to OCP photocycle is discussed in Section 6.

The lowest excited state (S_1 ($2^1 A_g^-$)) lifetime of hECN, which in carbonyl carotenoids is usually dramatically changed by the solvent polarity [54,55], was reported to be almost identical both in polar, and non-polar solvents, indicating that it exhibits the weakest polarity-induced effects observed so far among carbonyl carotenoids [52]. In another study, the absence of any polarity-induced shortening of the S_1 was observed in canthaxanthin (CAN) and echinenone (ECH), another two keto-carotenoids, which can bind to OCP [56]. On the other hand, the conformational change and hydrogen bonding via the carbonyl group of keto-carotenoid to OCP, results in dramatic shortening of S_1 in OCP^O to 3.3 ps, instead of 6.5 ps observed for hECN in solution [52]. This shortening is due to the change in β_1 orientation and, as a result, in effective conjugation length: in OCP^O it takes the *s-trans* configuration, while *s-cis* is the lowest energy configuration in solution [57]. The first time-resolved study on OCP claimed the S_1 state of hECN in OCP to decay with two time constants of 0.9 and 3.3 ps [52]. The multiexponential decay character of S_1 state, however, is currently unresolved and is important.

7.1. Intramolecular Charge Transfer

It has been reported by several groups that the excited state absorption of the $S_1 \rightarrow S_n$ and $ICT \rightarrow S_n$ transitions contribute to broad spectral features in the 550–700 nm range [8,35,52]. The intramolecular charge transfer (ICT) state is a characteristic feature of certain carbonyl carotenoids, and is readily observed in transient absorption spectra as a separate band appearing only in polar solvents [54,55]. However, keto-carotenoids with long ($N > 11$) conjugation, and with a conjugated keto-group located at the terminal ring, such as hECN, ECN or CAN, typically do not exhibit such a band [56]. Multiple studies, however, demonstrate the presence of the ICT band upon binding these carotenoids to OCP, indicating that the OCP binding pocket activates the ICT state [49–51]. Berera and co-workers were the first to assign 0.6 ps lifetime to ICT, due to the broad band in the 670 to 800 nm region, which becomes more pronounced in OCP^R . The second component (3.5 ps) was assigned to S_1 excited state, resolved both in OCP^O and OCP^R [49].

To exclude any OCP^O - OCP^R conversion during the measurements, the same authors later performed transient absorption studies on OCP^O and OCP^R , locked in their activation stages via freezing at 77 K. The results again demonstrated that both OCP forms show two intrinsic decay rates of the S_1/ICT state of hECN. Moreover, the decay lifetimes seem to be almost identical in both OCPs (2.0 and 7.5 ps in OCP^O and 2.3 and 7.6 ps in OCP^R) [51].

The predominantly ICT character has a lifetime of 2 ps and becomes more dominant in OCP^{R} , and another state with mainly S1 character has a lifetime of around 7.5 ps (Figure 8 model 1). While the spectroscopic features related to the ICT were reported to be even more pronounced in OCP^{R} [49,51] or RCP [50], no significant shortening of the overall lifetime in OCP^{R} versus OCP^{O} was observed [58].

7.2. Heterogeneity

Besides the role of the ICT state in the multiexponential character of S1, carotenoid heterogeneity once bound to OCP is another ongoing discussion in the literature. Slight differences in spectral and dynamical responses, obtained after excitation of OCP^{O} at 495 and 530 nm, were reported in 2005, where S1 state of hECN in OCP decayed with two time constants of 0.9 and 3.3 ps [52]. These lifetimes were originally explained by the presence of two populations of hECN in OCP, which differ in hydrogen bonding (Figure 8 model 2). In another study, the same authors suggested that the presence of two decay rates is associated with the coexistence of two forms of OCP, based on RT transient absorption studies, performed in VIS-NIR, where 0.9 ps is assigned to S1 of OCP^{R} and 3.3 ps to S1 of OCP^{O} [59]. By deconvoluting the absorption spectra of OCP^{O} and OCP^{R} , and separating S0–S2 and S2–S1 contributions, the authors estimated S1 energy of hECN in OCP^{O} and in OCP^{R} to be $14,700\text{ cm}^{-1}$ and $14,000\text{ cm}^{-1}$, respectively, indicating that significant changes in the vicinity of the conjugated carbonyl group occur upon activation [59]. However, transient absorption data measured on OCP binding zeaxanthin, which is incapable of OCP^{O} - OCP^{R} conversion [17], demonstrated that even for this OCP, which is locked in OCP^{O} state, two spectroscopically distinct zeaxanthins were identified [50]. The presence of two subpopulations within the same class of OCP was concluded from 77 K transient absorption studies, where one population has more enhance ICT character than the other [53]. Until now, the possible origin of this OCP heterogeneity has been unclear. For example, based on Resonance Raman spectra and DFT calculations, Maksimov et al. suggested that there are additional metastable configurations of the terminal ring, which retain hydrogen bonding to Trp and Tyr with varying C6–C7 dihedral angles (50° , 80° , 130°) between the polyene chain and the β 1-ring [33].

7.3. RCP

The S1 lifetime of hECN in RCP (RCP-hECH) is 5.5 ps, which is markedly longer than in OCP^{O} (3.3 ps), but close to the 6 ps obtained for hECN in organic solvent. This suggests that the binding of hECN to the C-terminal domain in OCP is primarily responsible for tuning its excited state properties [26]. In contrast to that, RCP-CAN has a very similar S1 lifetime to its OCP^{O} state. Furthermore, while RCP-CAN has an active ICT state [50], RCP-hECH does not [26]. In addition, the presence of ICT in RCP-CAN hardly affects its ultrafast kinetics, compared to OCP^{O} with the same bound carotenoid [57]. These observations seem to indicate that the energy landscape of keto-carotenoid in OCP has a carotenoid-specificity, and both domains (CTD, NTD) have important roles in providing this specificity.

7.4. Summary and Open Questions

While some authors assign the multiexponential character of the S1 excited state in OCP^{O} and OCP^{R} to OCP population heterogeneity [50,52,53], and others to the different contribution of ICT to the excited state kinetics [49–51], none of the mechanisms can relate these changes to physiological phenomena. For example, presence of ICT in RCP-CAN hardly affects its ultrafast kinetics, compared to OCP^{O} with the same carotenoid bound [50]. Furthermore, while RCP-CAN has an active ICT state, RCP-hECH [26] has not, but both serve as excellent quenchers of PBS fluorescence [15,22].

A further consideration is that changes in the S1 excited state lifetime in OCP^{R} , or in OCP^{O} with different H-bond conformations and/or β 1 ring torsions, is suggested by some studies not to contribute to a more efficient excited state quenching: The excited-state decay

of carotenoid S1 state is three orders of magnitude faster, compared to the excited state decay of bilin in phycobilisome. Therefore, any carotenoid would serve as an excellent quencher for a bilin, with essentially identical quenching efficiency.

These observations seem to suggest that excited state heterogeneity and ICT state are a consequence of the fine-tuning of S1 energy, through ring rotations and the conformation changes of keto-carotenoid bound to OCP. Due to the absence of unambiguous evidence that OCP quenches PBS energy directly, it raises an important question: *Could it be that these changes in OCP excited state properties reflect structural changes, which are important for OCP binding to promote indirect quenching?*

Another question which requires more in-depth study of the reasons and consequences of carotenoid-specificity on OCP excited state properties is: *Does it affect light activation and/or antenna quenching and, if it does, which domains, amino acids, and bonds have an important role in these processes?*

8. General Conclusions and Future Prospects

Over the last 15 years, since OCP structure was first resolved (which at the time was a protein of unknown function), many advances in our understanding of its role in cyanobacterial photoprotection have been achieved.

Overall, upon light activation, NTD and CTD are separated and carotenoid is translocated into NTD [16,21]. Various amino acids (e.g., Tyr201, Trp288 or Trp41) play an active role in the light activation process [17–19]; however, the stage at which they contribute to the photocycle is still unclear. Different photocycle intermediates were observed spectroscopically, from a picosecond to a second timescale [33–36]. There are still structural data missing to confirm any of the proposed models of the OCP photocycle; therefore, interpretations are provisional and based on spectroscopic evidence only. Different hypothesis about the trigger of light activation have been also put forward [15,16,18,19,35,41,45]. Most suggest that the H-bond rupture is the primary photoevent [15,16,18,19,35,41]; however, of all the hypotheses proposed, high-resolution structural data is urgently needed to resolve the triggering mechanism.

To summarize, many questions regarding the mechanism of OCP light activation remain unanswered, or are under debate. We believe that the current key topics regarding OCP light activation are:

1. **Trigger mechanism:** Based on either structural or spectroscopic studies, proposed candidates for the trigger of OCP light activation are (1) β 1-ring flip, due to photoisomerization; (2) enolization of β 1-ring and protein moiety; (3) H-bond rupture due to a “hot” excited state; (4) out-of-plane motions in β 2-ring. None of these mechanisms were exclusively supported in the literature, and there many results pointing in favor of different models. Unambiguously resolving the trigger and location of OCP light activation is essential to understand, and potentially controlling the OCP activation mechanism. The combination of ultrafast time-resolved spectroscopy, and structural time-resolved techniques, should be exploited to investigate this point.
2. **Intermediates:** To fully understand the process and potential gain control of OCP light activation, we need to resolve all OCP intermediate states, and their lifetimes. For example, there are spectroscopic results suggesting that OCP reaches its red state in less than 0.2 μ s, before major structural reorganizations (which seem to be mainly localized in NTD), while other results suggest that this process is 50 times slower, and happens after NTD reorganizations. It is also not clear when H-bond rupture occurs, what its spectroscopic signature is, and its role within light activation. Other intermediates and lifetimes of OCP^O-OCP^R-OCP^O photocycle still need to be either resolved or confirmed, based on spectroscopic characters and more advanced structural insights.
3. **Carotenoid/OCP specificity:** Spectroscopic studies suggest keto-carotenoid specificity, affecting energetic landscape and excited state kinetics of OCP and RCP. Furthermore, genomic data are beginning to hint of a wider role for OCP homologs beyond

photoprotection, possibly within other types of adaptation to changing environment. Therefore, it is important to elucidate whether the trigger and the mechanism of OCP light activation are universal, or if there is some carotenoid/OCP-specificity.

4. **NPQ mechanism:** The biological function of OCP is established as a fluorescence quenching of the phycobilisome light harvesting complexes (NPQ); however, the transfer mechanism is unknown. Neither Förster theory or Dexter theory support a mechanism of excitation energy transfer from allophycocyanin (APC), to the S_1 ($2^1 A_g^-$) state of OCP^R ; therefore, a charge transfer mechanism has been proposed [11]. Potential mechanisms include a dipole-quadrupole interaction, a breakdown of C_{2h} symmetry, or intensity borrowing from the S_2 ($1^1 B_u^+$) state through higher vibrational levels of the S_1 ($2^1 A_g^-$) state. An evaluation of the possible mechanism requires a measurement of the energy transfer rate, which is proportional to the square of the coupling strength, $K_{ET} = 1.18 |V|^2 J$ (V is the coupling constant, cm^{-1} , and J is the spectral overlap integral). In principle, the rate can be measured from an equilibration experiment of OCP^R with APC_{660} phycobilisome antenna pigment, that can be prepared by illumination of OCP^O to form OCP^R , which will bind APC [60]. The rate constant could be determined by ultrafast spectroscopy of APC_{660} - OCP^R complex, in order to measure the overlap integral from high-sensitivity fluorescence measurements. Additionally, direct population of the S_1 ($2^1 A_g^-$) state could be achieved by two-photon absorption. While the S_0 ($1^1 A_g^-$) \rightarrow S_1 ($2^1 A_g^-$) state is one-photon disallowed, the transition is two-photon allowed using ~ 1.2 – $1.3 \mu m$ wavelength excitation. Similar experiments have been successfully demonstrated for the Car (S1)-BChl (S1) transfer in B800–B850 complexes [61].

Gaining control over OCP light activation and, therefore, cyanobacterial light-harvesting, could provide new inspiration for scientists on improving photosynthesis productivity. Understanding and controlling the mechanism of OCP light activation could also potentially revolutionize the field of optogenetics. Currently, optogenetics sensors based on carotenoids do not exist. However, they are very attractive candidates for such applications, due to their abundance in nature, non-toxicity, light and temperature stability [62].

Author Contributions: Conceptualization, V.U.C. and J.J.v.T.; writing—review and editing, V.U.C. and J.J.v.T.; visualization, V.U.C. All authors have read and agreed to the published version of the manuscript.

Funding: This project was supported by the EMBO long-term fellowship (EMBO ALTF 244-2017) and has received funding from the European Union Horizon 2020 research and innovation programme, under the Marie Skłodowska-Curie grant (agreement No. 839389) to V.C. This work was supported by the Leverhulme Trust award RPG-2018-372.

Institutional Review Board Statement: Not applicable.

Data Availability Statement: Not applicable.

Conflicts of Interest: The authors declare no conflict of interest.

Abbreviations

APC, allophycocyanin; CD, circular dichroism; CTD, C-terminal domain; CAN, canthaxanthin; DFT, density functional theory; ECN, echinenone; EET, excitation energy transfer; ESA, excited state absorption; FTIR, Fourier-transform infrared spectroscopy; HDX-MS, hydrogen deuterium exchange mass spectrometry; hECN, 3-hydroxyl-echinenone; ICT, intramolecular charge transfer; MALDI-MS, matrix-assisted laser desorption/ionization mass spectrometry; MW, molecular weight; NTD, N-terminal domain; NTE, N-terminal extension; NTF2, Nuclear Transport Factor-2; NPQ, non-photochemical quenching; OCP, Orange Carotenoid Protein; OD, optical density; PBS, phycobilisome; RCP, red carotenoid protein, containing N-terminal domain only; SAXS, small angle X-ray scattering; SEC, size exclusion chromatography; XF-MS, X-ray footprinting with mass spectrometry.

References

1. Ernst, O.P.; Lodowski, D.T.; Elstner, M.; Hegemann, P.; Brown, L.S.; Kandori, H. Microbial and animal rhodopsins: Structures, functions, and molecular mechanisms. *Chem. Rev.* **2014**, *114*, 126–163. [[CrossRef](#)] [[PubMed](#)]
2. Nagy, F.; Schäfer, E. Phytochromes control photomorphogenesis by differentially regulated, interacting signaling pathways in higher plants. *Annu. Rev. Plant Biol.* **2002**, *53*, 329–355. [[CrossRef](#)] [[PubMed](#)]
3. Christie, J.M.; Blackwood, L.; Petersen, J.; Sullivan, S. Plant flavoprotein photoreceptors. *Plant Cell Physiol.* **2015**, *56*, 401–413. [[CrossRef](#)]
4. Horton, P.; Hague, A. Studies on the induction of chlorophyll fluorescence in isolated barley protoplasts. IV. Resolution of non-photochemical quenching. *Biochim. Biophys. Acta-Bioenerg.* **1988**, *932*, 107–115. [[CrossRef](#)]
5. Adams, W.W.; Demmig-Adams, B. Operation of the xanthophyll cycle in higher plants in response to diurnal changes in incident sunlight. *Planta* **1992**, *186*, 390–398. [[CrossRef](#)]
6. Kirilovsky, D.; Kerfeld, C.A. The Orange Carotenoid Protein: A blue-green light photoactive protein. *Photochem. Photobiol. Sci.* **2013**, *2*, 1135–1143. [[CrossRef](#)] [[PubMed](#)]
7. Kerfeld, C.A.; Sawaya, M.R.; Brahmandam, V.; Cascio, D.; Ho, K.K.; Trevithick-Sutton, C.C.; Krogmann, D.W.; Yeates, T.O. The crystal structure of a cyanobacterial water-soluble carotenoid binding protein. *Structure* **2003**, *11*, 55–65. [[CrossRef](#)]
8. Wilson, A.; Punginelli, C.; Gall, A.; Bonetti, C.; Alexandre, M.; Routaboul, J.M.; Kerfeld, C.A.; van Grondelle, R.; Robert, B.; Kennis, J.T.; et al. A photoactive carotenoid protein acting as light intensity sensor. *Proc. Natl. Acad. Sci. USA* **2008**, *105*, 12075–12080. [[CrossRef](#)]
9. Gwizdala, M.; Wilson, A.; Kirilovsky, D. In vitro reconstitution of the cyanobacterial photoprotective mechanism mediated by the Orange Carotenoid Protein in *Synechocystis* PCC 6803. *Plant Cell* **2011**, *23*, 2631–2643. [[CrossRef](#)]
10. Maksimov, E.G.; Schmitt, F.J.; Shirshin, E.A.; Svirin, M.D.; Elanskaya, I.V.; Friedrich, T.; Fadeev, V.V.; Paschenko, V.Z.; Rubin, A.B. The time course of non-photochemical quenching in phycobilisomes of *Synechocystis* sp. PCC6803 as revealed by picosecond time-resolved fluorimetry. *Biochim. Biophys. Acta-Bioenerg.* **2014**, *1837*, 1540–1547. [[CrossRef](#)]
11. Tian, L.; van Stokkum, I.H.M.; Koehorst, R.B.M.; Jongerius, A.; Kirilovsky, D.; van Amerongen, H. Site, rate, and mechanism of photoprotective quenching in cyanobacteria. *J. Am. Chem. Soc.* **2011**, *133*, 18304–18311. [[CrossRef](#)] [[PubMed](#)]
12. Harris, D.; Tal, O.; Jallet, D.; Wilson, A.; Kirilovsky, D.; Adir, N. Orange carotenoid protein burrows into the phycobilisome to provide photoprotection. *Proc. Natl. Acad. Sci. USA* **2016**, *113*, E1655–E1662. [[CrossRef](#)] [[PubMed](#)]
13. Muzzopappa, F.; Kirilovsky, D. Changing Color for Photoprotection: The Orange Carotenoid Protein. *Trends Plant Sci.* **2020**, *25*, 92–104. [[CrossRef](#)] [[PubMed](#)]
14. Punginelli, C.; Wilson, A.; Routaboul, J.M.; Kirilovsky, D. Influence of zeaxanthin and echinenone binding on the activity of the orange carotenoid protein. *Biochim. Biophys. Acta-Bioenerg.* **2009**, *1787*, 280–288. [[CrossRef](#)] [[PubMed](#)]
15. Leverenz, R.L.; Sutter, M.; Wilson, A.; Gupta, S.; Thurotte, A.; de Carbon, C.B.; Petzold, C.J.; Ralston, C.; Perreau, F.; Kirilovsky, D.; et al. A 12 Å carotenoid translocation in a photoswitch associated with cyanobacterial photoprotection. *Science* **2015**, *348*, 1463–1466. [[CrossRef](#)]
16. Bandara, S.; Ren, Z.; Lu, L.; Zeng, X.; Shin, H.; Zhao, K.-H.H.; Yang, X. Photoactivation mechanism of a carotenoid-based photoreceptor. *Proc. Natl. Acad. Sci. USA* **2017**, *114*, 6286–6291. [[CrossRef](#)]
17. Wilson, A.; Punginelli, C.; Couturier, M.; Perreau, F.; Kirilovsky, D. Essential role of two tyrosines and two tryptophans on the photoprotection activity of the Orange Carotenoid Protein. *Biochim. Biophys. Acta-Bioenerg.* **2011**, *1807*, 293–301. [[CrossRef](#)]
18. Wilson, A.; Gwizdala, M.; Mezzetti, A.; Alexandre, M.; Kerfeld, C.A.; Kirilovsky, D. The essential role of the N-terminal domain of the orange carotenoid protein in cyanobacterial photoprotection: Importance of a positive charge for phycobilisome binding. *Plant Cell* **2012**, *24*, 1972–1983. [[CrossRef](#)]
19. Wilson, A.; Kinney, J.N.; Zwart, P.H.; Punginelli, C.; D’Haene, S.; Perreau, F.; Klein, M.G.; Kirilovsky, D.; Kerfeld, C.A. Structural determinants underlying photoprotection in the photoactive orange carotenoid protein of cyanobacteria. *J. Biol. Chem.* **2010**, *285*, 18364–18375. [[CrossRef](#)]
20. Wu, Y.P.; Krogmann, D.W. The orange carotenoid protein of *Synechocystis* PCC 6803. *Biochim. Biophys. Acta-Bioenerg.* **1997**, *1322*, 1–7. [[CrossRef](#)]
21. Gupta, S.; Guttman, M.; Leverenz, R.L.; Zhumadilova, K.; Pawlowski, E.G.; Petzold, C.J.; Lee, K.K.; Ralston, C.Y.; Kerfeld, C.A. Local and global structural drivers for the photoactivation of the orange carotenoid protein. *Proc. Natl. Acad. Sci. USA* **2015**, *112*, E5567–E5574. [[CrossRef](#)] [[PubMed](#)]
22. Leverenz, R.L.; Jallet, D.; de Li, M.; Mathies, R.A.; Kirilovsky, D.; Kerfeld, C.A. Structural and functionalmodularity of the orange carotenoid protein: Distinct roles for the N- and C-terminal domains in cyanobacterial photoprotection. *Plant Cell* **2014**, *26*, 426–437. [[CrossRef](#)] [[PubMed](#)]
23. Chai, Y.G.; Song, P.S.; Cordonnier, M.M.; Pratt, L.H. A Photoreversible Circular Dichroism Spectral Change in Oat Phytochrome Is Suppressed by a Monoclonal Antibody That Binds near Its N-Terminus and by Chromophore Modification. *Biochemistry* **1987**, *26*, 4947–4952. [[CrossRef](#)] [[PubMed](#)]
24. Shimizu, N.; Imamoto, Y.; Harigai, M.; Kamikubo, H.; Yamazaki, Y.; Kataoka, M. pH-dependent equilibrium between long lived near-UV intermediates of photoactive yellow protein. *J. Biol. Chem.* **2006**, *281*, 4318–4325. [[CrossRef](#)] [[PubMed](#)]

25. Liu, H.; Zhang, H.; King, J.D.; Wolf, N.R.; Prado, M.; Gross, M.L.; Blankenship, R.E. Mass spectrometry footprinting reveals the structural rearrangements of cyanobacterial orange carotenoid protein upon light activation. *Biochim. Biophys. Acta-Bioenerg.* **2014**, *1837*, 1955–1963. [[CrossRef](#)]
26. Chábera, P.; Durchan, M.; Shih, P.M.; Kerfeld, C.A.; Polívka, T. Excited-state properties of the 16kDa red carotenoid protein from *Arthrospira maxima*. *Biochim. Biophys. Acta-Bioenerg.* **2011**, *1807*, 30–35. [[CrossRef](#)]
27. King, J.D.; Liu, H.; He, G.; Orf, G.S.; Blankenship, R.E. Chemical activation of the cyanobacterial orange carotenoid protein. *FEBS Lett.* **2014**, *588*, 4561–4565. [[CrossRef](#)]
28. Liu, H.J.; Zhang, H.; Niedzwiedzki, D.M.; Prado, M.; He, G.N.; Gross, M.L.; Blankenship, R.E. Phycobilisomes Supply Excitations to Both Photosystems in a Megacomplex in Cyanobacteria. *Science* **2013**, *342*, 1104–1107. [[CrossRef](#)]
29. Kennis, J.T.M.; Crosson, S.; Gauden, M.; van Stokkum, I.H.M.; Moffat, K.; van Grondelle, R. Primary reactions of the LOV2 domain of phototropin, a plant blue-light photoreceptor. *Biochemistry* **2003**, *42*, 3385–3392. [[CrossRef](#)]
30. Gauden, M.; Yeremenko, S.; Laan, W.; van Stokkum, I.H.M.; Ihalaainen, J.A.; van Grondelle, R.; Hellingwerf, K.J.; Kennis, J.T.M. Photocycle of the flavin-binding photoreceptor AppA, a bacterial transcriptional antirepressor of photosynthesis genes. *Biochemistry* **2005**, *44*, 3653–3662. [[CrossRef](#)]
31. Hutchison, C.D.M.; Kaucikas, M.; Tenboer, J.; Kupitz, C.; Moffat, K.; Schmidt, M.; van Thor, J.J. Photocycle populations with femtosecond excitation of crystalline photoactive yellow protein. *Chem. Phys. Lett.* **2016**, *654*, 63–71. [[CrossRef](#)]
32. van Thor, J.J.; Gensch, T.; Hellingwerf, K.J.; Johnson, L.N. Phototransformation of green fluorescent protein with UV and visible light leads to decarboxylation of glutamate 222. *Nat. Struct. Biol.* **2002**, *9*, 37–41. [[CrossRef](#)]
33. Maksimov, E.G.; Shirshin, E.A.; Sluchanko, N.N.; Zlenko, D.V.; Parshina, E.Y.; Tsoraev, G.V.; Klementiev, K.E.; Budylin, G.S.; Schmitt, F.-J.; Friedrich, T.; et al. The Signaling State of Orange Carotenoid Protein. *Biophys. J.* **2015**, *109*, 595–607. [[CrossRef](#)] [[PubMed](#)]
34. Maksimov, E.G.; Sluchanko, N.N.; Slonimskiy, Y.B.; Slutskaya, E.A.; Stepanov, A.V.; Argentova-Stevens, A.M.; Shirshin, E.A.; Tsoraev, G.V.; Klementiev, K.E.; Slatinskaya, O.V.; et al. The photocycle of orange carotenoid protein conceals distinct intermediates and asynchronous changes in the carotenoid and protein components. *Sci. Rep.* **2017**, *7*, 1–12. [[CrossRef](#)] [[PubMed](#)]
35. Konold, P.E.; van Stokkum, I.H.M.; Muzzopappa, F.; Wilson, A.; Groot, M.L.; Kirilovsky, D.; Kennis, J.T.M. Photoactivation Mechanism, Timing of Protein Secondary Structure Dynamics and Carotenoid Translocation in the Orange Carotenoid Protein. *J. Am. Chem. Soc.* **2019**, *141*, 520–530. [[CrossRef](#)]
36. Mezzetti, A.; Alexandre, M.; Thurotte, A.; Wilson, A.; Gwizdala, M.; Kirilovsky, D. Two-Step Structural Changes in Orange Carotenoid Protein Photoactivation Revealed by Time-Resolved Fourier Transform Infrared Spectroscopy. *J. Phys. Chem. B* **2019**, *123*, 3259–3266. [[CrossRef](#)]
37. Warren, M.M.; Kaucikas, M.; Fitzpatrick, A.; Champion, P.; Sage, J.T.; van Thor, J.J. Ground-state proton transfer in the photoswitching reactions of the fluorescent protein Dronpa. *Nat. Commun.* **2013**, *4*, 1461. [[CrossRef](#)]
38. Warren, C.K.; Weedon, B.C.L. 804. Carotenoids and related compounds. Part VII. Synthesis of canthaxanthin and echinenone. *J. Chem. Soc.* **1958**, 3986–3993. [[CrossRef](#)]
39. Kish, E.; Pinto, M.M.M.; Kirilovsky, D.; Spezia, R.; Robert, B. Echinenone vibrational properties: From solvents to the orange carotenoid protein. *Biochim. Biophys. Acta-Bioenerg.* **2015**, *1847*, 1044–1054. [[CrossRef](#)]
40. Gurchiek, J.K.; Bao, H.; Domínguez-Martín, M.A.; McGovern, S.E.; Marquardt, C.E.; Roscioli, J.D.; Ghosh, S.; Kerfeld, C.A.; Beck, W.F. Fluorescence and Excited-State Conformational Dynamics of the Orange Carotenoid Protein. *J. Phys. Chem. B* **2018**, *122*, 1792–1800. [[CrossRef](#)]
41. Bondanza, M.; Cupellini, L.; Lipparini, F.; Mennucci, B. The Multiple Roles of the Protein in the Photoactivation of Orange Carotenoid Protein. *Chem* **2020**, *6*, 187–203. [[CrossRef](#)]
42. Pande, K.; Hutchison, C.D.M.; Groenhof, G.; Aquila, A.; Robinson, J.S.; Tenboer, J.; Basu, S.; Boutet, S.; DePonte, D.P.; Liang, M.N.; et al. Femtosecond structural dynamics drives the trans/cis isomerization in photoactive yellow protein. *Science* **2016**, *352*, 725–729. [[CrossRef](#)] [[PubMed](#)]
43. Schmidt, M.; Krasselt, A.; Reuter, W. Local protein flexibility as a prerequisite for reversible chromophore isomerization in α -phycoerythrocyanin. *Biochim. Biophys. Acta-Proteins Proteom.* **2006**, *1764*, 55–62. [[CrossRef](#)]
44. Schoenlein, R.W.; Peteanu, L.A.; Mathies, R.A.; Shank, C.V. The first step in vision: Femtosecond isomerization of rhodopsin. *Science* **1991**, *254*, 412–415. [[CrossRef](#)]
45. Liguori, N.; Xu, P.; van Stokkum, I.H.M.; van Oort, B.; Lu, Y.; Karcher, D.; Bock, R.; Croce, R. Different carotenoid conformations have distinct functions in light-harvesting regulation in plants. *Nat. Commun.* **2017**, *8*, 1994. [[CrossRef](#)] [[PubMed](#)]
46. Balevičius, V.; Wei, T.; di Tommaso, D.; Abramavicius, D.; Hauer, J.; Polívka, T.; Duffy, C.D.P. The full dynamics of energy relaxation in large organic molecules: From photo-excitation to solvent heating. *Chem. Sci.* **2019**, *10*, 4792–4804. [[CrossRef](#)] [[PubMed](#)]
47. Khan, T.; Kuznetsova, V.; Dominguez-Martin, M.A.; Kerfeld, C.A.; Polívka, T. UV Excitation of Carotenoid Binding Proteins OCP and HCP: Excited-State Dynamics and Product Formation. *ChemPhotoChem* **2022**, *6*, e202100194. [[CrossRef](#)]
48. Niziński, S.; Wilson, A.; Uriarte, L.M.; Ruckebusch, C.; Andreeva, E.A.; Schlichting, I.; Colletier, J.-P.; Kirilovsky, D.; Burdzinski, G.; Sliwa, M. Unifying Perspective of the Ultrafast Photodynamics of Orange Carotenoid Proteins from Synechocystis: Peril of High-Power Excitation, Existence of Different S* States, and Influence of Tagging. *JACS Au* **2022**, *2*, 1084–1095. [[CrossRef](#)]

49. Berera, R.; van Stokkum, I.H.M.; Gwizdala, M.; Wilson, A.; Kirilovsky, D.; van Grondelle, R. The photophysics of the orange carotenoid protein, a light-powered molecular switch. *J. Phys. Chem. B* **2012**, *116*, 2568–2574. [[CrossRef](#)]
50. Šlouf, V.; Kuznetsova, V.; Fuciman, M.; de Carbon, C.B.; Wilson, A.; Kirilovsky, D.; Polívka, T. Ultrafast spectroscopy tracks carotenoid configurations in the orange and red carotenoid proteins from cyanobacteria. *Photosynth. Res.* **2017**, *131*, 105–117. [[CrossRef](#)]
51. Berera, R.; Gwizdala, M.; van Stokkum, I.H.; Kirilovsky, D.; van Grondelle, R. Excited states of the inactive and active forms of the orange carotenoid protein. *J. Phys. Chem. B* **2013**, *117*, 9121–9128. [[CrossRef](#)] [[PubMed](#)]
52. Polívka, T.; Kerfeld, C.A.; Pascher, T.; Sundström, V. Spectroscopic properties of the carotenoid 3'-hydroxyechinenone in the orange carotenoid protein from the cyanobacterium *Arthrospira maxima*. *Biochemistry* **2005**, *44*, 3994–4003. [[CrossRef](#)] [[PubMed](#)]
53. Niedzwiedzki, D.M.; Liu, H.; Blankenship, R.E. Excited state properties of 3'-hydroxyechinenone in solvents and in the orange carotenoid protein from *Synechocystis* sp. PCC 6803. *J. Phys. Chem. B* **2014**, *118*, 6141–6149. [[CrossRef](#)] [[PubMed](#)]
54. Frank, H.A.; Bautista, J.A.; Josue, J.; Pendon, Z.; Hiller, R.G.; Sharples, F.P.; Gosztola, D.; Wasielewski, M.R. Effect of the Solvent Environment on the Spectroscopic Properties and Dynamics of the Lowest Excited States of Carotenoids. *J. Phys. Chem. B* **2000**, *104*, 4569–4577. [[CrossRef](#)]
55. Zigmantas, D.; Hiller, R.G.; Sharples, F.P.; Frank, H.A.; Sundström, V.; Polívka, T. Effect of a conjugated carbonyl group on the photophysical properties of carotenoids. *Phys. Chem. Chem. Phys.* **2004**, *6*, 3009–3016. [[CrossRef](#)]
56. Chábera, P.; Fuciman, M.; Híbek, P.; Polívka, T. Effect of carotenoid structure on excited-state dynamics of carbonyl carotenoids. *Phys. Chem. Chem. Phys.* **2009**, *11*, 8795–8803. [[CrossRef](#)]
57. Fujisawa, T.; Leverenz, R.L.; Nagamine, M.; Kerfeld, C.A.; Unno, M. Raman Optical Activity Reveals Carotenoid Photoactivation Events in the Orange Carotenoid Protein in Solution. *J. Am. Chem. Soc.* **2017**, *139*, 10456–10460. [[CrossRef](#)]
58. de Re, E.; Schlau-Cohen, G.S.; Leverenz, R.L.; Huxter, V.M.; Oliver, T.A.A.; Mathies, R.A.; Fleming, G.R. Insights into the structural changes occurring upon photoconversion in the orange carotenoid protein from broadband two-dimensional electronic spectroscopy. *J. Phys. Chem. B* **2014**, *118*, 5382–5389. [[CrossRef](#)]
59. Polívka, T.; Chabera, P.; Kerfeld, C.A. Carotenoid-protein interaction alters the S(1) energy of hydroxyechinenone in the Orange Carotenoid Protein. *Biochim. Biophys. Acta-Bioenerg.* **2013**, *1827*, 248–254. [[CrossRef](#)]
60. Tian, L.; Gwizdala, M.; van Stokkum, I.H.; Koehorst, R.B.; Kirilovsky, D.; van Amerongen, H. Picosecond kinetics of light harvesting and photoprotective quenching in wild-type and mutant phycobilisomes isolated from the cyanobacterium *Synechocystis* PCC 6803. *Biophys. J.* **2012**, *102*, 1692–1700. [[CrossRef](#)]
61. Walla, P.J.; Linden, P.A.; Hsu, C.-P.; Scholes, G.D.; Fleming, G.R. Femtosecond dynamics of the forbidden carotenoid S1 state in light-harvesting complexes of purple bacteria observed after two-photon excitation. *Proc. Natl. Acad. Sci. USA* **2000**, *97*, 10808–10813. [[CrossRef](#)] [[PubMed](#)]
62. Ngamwonglumlert, L.; Devahastin, S.; Chiewchan, N. Natural colorants: Pigment stability and extraction yield enhancement via utilization of appropriate pretreatment and extraction methods. *Crit. Rev. Food Sci. Nutr.* **2017**, *57*, 3243–3259. [[CrossRef](#)] [[PubMed](#)]